FRONTLINE

Frontline

Somatic mutations and affinity maturation are impaired by excessive numbers of T follicular helper cells and restored by Treg cells or memory T cells

Silvia Preite[1], Dirk Baumjohann[1], Mathilde Foglierini[1], Camilla Basso[1], Francesca Ronchi[1], Blanca M. Fernandez Rodriguez[1], Davide Corti[1], Antonio Lanzavecchia[1,2] and Federica Sallusto[1]

[1] Institute for Research in Biomedicine, Università della Svizzera Italiana, Bellinzona, Switzerland
[2] Institute of Microbiology, ETH Zürich, Zurich, Switzerland

We previously reported that *Cd3e*-deficient mice adoptively transferred with CD4^{+} T cells generate high numbers of T follicular helper (Tfh) cells, which go on to induce a strong B-cell and germinal center (GC) reaction. Here, we show that in this system, GC B cells display an altered distribution between the dark and light zones, and express low levels of activation-induced cytidine deaminase. Furthermore, GC B cells from *Cd3e*^{−/−} mice accumulate fewer somatic mutations as compared with GC B cells from wild-type mice, and exhibit impaired affinity maturation and reduced differentiation into long-lived plasma cells. Reconstitution of *Cd3e*^{−/−} mice with regulatory T (Treg) cells restored Tfh-cell numbers, GC B-cell numbers and B-cell distribution within dark and light zones, and the rate of antibody somatic mutations. Tfh-cell numbers and GC B-cell numbers and dynamics were also restored by pre-reconstitution of *Cd3e*^{−/−} mice with *Cxcr5*^{−/−} Treg cells or non-regulatory, memory CD4^{+} T cells. Taken together, these findings underline the importance of a quantitatively regulated Tfh-cell response for an efficient and long-lasting serological response.

Keywords: Antibodies · Germinal center · Lymphopenia · Somatic hypermutation · Tfh cell

Additional supporting information may be found in the online version of this article at the publisher's web-site

Introduction

T follicular helper (Tfh) cells are specialized Th cells that reside in the B-cell follicle and provide help to B cells through co-stimulatory molecules and cytokines [1]. Upon antigen activation, B cells can give rise to short-lived antibody-secreting cells (ASCs), that generate the extra-follicular response, or they can re-enter the B-cell follicle to form germinal centers (GCs) [2]. Tfh cells play an essential role for both the initiation and maintenance of the GC reaction, in which class-switch recombination and somatic hypermutation (SHM) lead to the generation of high-affinity antibodies produced by long-lived plasma cells and memory B cells [3].

Based on histological assessment, the GC has been divided into a dark zone (DZ) and a light zone (LZ) where distinct processes take place. According to the current model [2], B-cell selection occurs in the LZ and relies on affinity-dependent retrieval of antigen from follicular dendritic cells and cognate engagement between GC B cells and Tfh cells. Subsequently, GC B cells receive

signals from Tfh cells to migrate toward the DZ to proliferate and to initiate activation-induced cytidine deaminase (AID)-driven somatic mutations. According to this model, Tfh cells are critical players in the selection of high-affinity B-cell clones since they control the iterative cycles of GC B cells from the DZ to the LZ [4]. However, there is no information on how the magnitude of the Tfh-cell response impacts on the GC dynamics and, in particular, on the process of SHM.

Several cell-intrinsic and cell-extrinsic mechanisms control Tfh-cell homeostasis [5, 6]. Recent studies unveiled the existence of a subset of Bcl6^{+} Foxp3^{+} T follicular regulatory cells (Tfr) that originate from thymic-derived (Helios^{+}) nTreg cells and display an intermediate phenotype between Treg and Tfh cells [7]. Tfr cells, which have been described as CXCR5^{hi} PD1^{hi} ICOS^{+} CCR7^{−} CD25^{int}, have been shown to suppress the GC reaction, possibly acting in the B-cell follicles on Tfh and/or GC B cells [7]. However, the role of Tfr cells and the impact of Tfh-cell numbers on the selection of mutated high-affinity B cells remains to be investigated in more detail.

We recently reported that the magnitude of the mouse Tfh-cell response is dictated by the amount of antigen and directly correlates with the magnitude of the GC B-cell response [8]. These findings were obtained in immunocompetent wild-type hosts (WT) as well as in lymphopenic hosts. We noticed, however, that Tfh cells, which are generated in high numbers in lymphopenic mice, become dysfunctional and fail to provide help to sustain long-term antigen-specific antibodies [8]. In the current study, we demonstrate that, as a consequence of the dysfunctional Tfh cell response, GC B cell-dynamics between LZ and DZ are altered, leading to a lack of antibody affinity maturation and reduced number of somatic mutations in the VH genes. We also found that reconstitution of lymphopenic mice with CXCR5-sufficient and CXCR5-deficient Treg cells, as well as non-regulatory memory CD4 T cells, restrained expansion of Tfh and GC B cells, and restored GC B-cell dynamics and generation of highly mutated, high-affinity antibodies.

Results

Impaired antibody affinity maturation in *Cd3e*^{−/−} mice adoptively transferred with OT-II cells

In this study, we used T-cell-deficient *Cd3e*^{−/−} mice that in steady state have a normal B-cell compartment and lymphoid organs [9], basal serum IgM levels comparable to WT mice, but reduced levels of IgG1, IgG2b, IgG2c, and IgA, and increased levels of IgG3 (Supporting Information Fig. S1A–D). These mice mounted a normal IgM and IgG3 response to the T-independent antigen NP-Ficoll (data not shown), but failed to make an IgG1 response to the T-dependent antigen ovalbumin (OVA) (Supporting Information Fig. S1E).

Cd3e^{−/−} or WT mice were transferred with OVA-specific TCR-tg OT-II CD4^{+} T cells (OT-II→*Cd3e*^{−/−} and OT-II→WT, respectively) and immunized with OVA in alum. As previously reported [8],

OT-II cells expanded to a much greater extent in *Cd3e*^{−/−} mice as compared to WT mice and differentiated to a greater extent into CXCR5^{+} PD1^{+} ICOS^{+} Tfh cells, expressing high levels of Bcl6 and producing high amounts of IL-21 and IFN-γ (Ref. [8] and Supporting Information Fig. S2A–C). In both groups of mice, FAS[+]GL7^{+} GC B cells increased on day +7, whereas on day +21 they slightly decreased in WT mice and further increased in *Cd3e*^{−/−} mice (Fig. 1A, left panel). While plasma cells were only transiently increased on day +7 in OT-II→WT mice, they were present in high numbers in the spleen of OT-II→*Cd3e*^{−/−} mice on day +7 and +21 (Fig. 1A, right panel). Histological analysis of splenic sections of immunized *Cd3e*^{−/−} recipients showed that proliferating OT-II cells were initially localized in the vacant T-cell zones and at the border of B-cell follicles while they increasingly accumulated in GCs at later time points (Fig. 1B), which coincided with their expression of Tfh-cell markers. In splenic sections, GCs were clearly detected on day +10 in both groups of mice, while at later time points (day +13) they were greatly enlarged in *Cd3e*^{−/−} as compared to WT mice (Fig. 1B), consistent with the more sustained proliferation of OT-II cells and GC B cells observed in these mice.

To assess affinity maturation of the induced antibody response, OT-II→WT and OT-II→*Cd3e*^{−/−} mice were immunized i.p. with NP$_{19}$-OVA and the kinetics of IgG and IgG1 antibodies that bound to NP$_{23}$-BSA (as a measure of total NP-specific antibodies) and NP$_3$-BSA (as a measure of high-affinity NP-specific antibodies) were determined by ELISA (Fig. 1C). Strikingly, when compared to WT recipients, the total anti-NP antibody response in *Cd3e*^{−/−} recipients increased more rapidly and reached higher levels by day +15, but decreased at later time points. A similar and even more striking pattern was observed for high-affinity anti-NP$_3$ antibodies, which peaked on day +10 and decreased thereafter in *Cd3e*^{−/−} recipients, while it steadily increased up to day +25 in WT recipients (Fig. 1C). Thus, while the NP$_3$/NP$_{23}$ ratio increased in OT-II→WT, indicative of affinity maturation in the antibody response, it remained at low and variable levels in OT-II→*Cd3e*^{−/−} mice (Fig. 1D).

We next measured splenic and bone marrow ASCs that represent short-lived and long-lived plasma cells, respectively [10]. On day +25 after immunization with NP$_{19}$-OVA, both total NP$_{23}$-specific and high-affinity NP$_3$-specific plasma cells were present at much higher number in the spleen of *Cd3e*^{−/−} mice as compared to WT mice (Fig. 1E, left panel). In striking contrast, there were fewer NP$_{23}$-specific plasma cells in the bone marrow of *Cd3e*^{−/−} mice as compared to WT mice, and NP$_3$-specific high-affinity plasma cells were almost absent (Fig. 1E, right panel), suggesting that most antigen-stimulated B cells differentiated into short-lived plasma cells. This notion is corroborated by the finding that in *Cd3e*^{−/−} mice Tfh cells expressed high levels of CXCR4 and low levels of PSGL-1 (Supporting Information Fig. S2D), a phenotype that has been associated with Tfh cells supporting extrafollicular plasma cells [11, 12]. It should be noted that total polyclonal IgG1^{+} ASCs were found in high numbers in the spleen and bone marrow of immunized *Cd3e*^{−/−} mice (Fig. 1F), consistent with our previous finding that Tfh cells in lymphopenic environments can
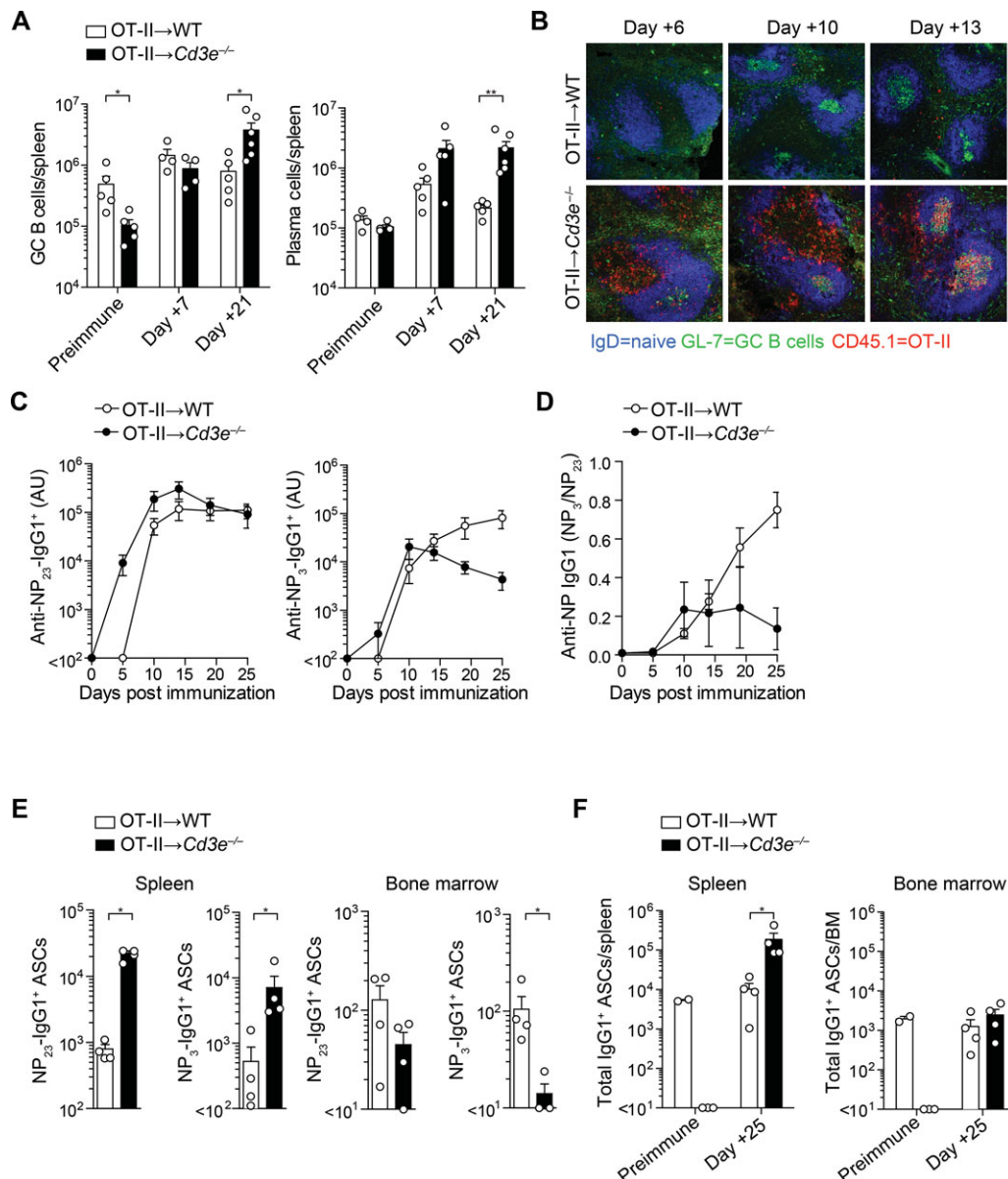
Figure 1. High numbers of Tfh cells induce a strong GC reaction, which does not lead to the generation of high-affinity antibodies. (A–F) WT or $Cd3e^{-/-}$ mice adoptively transferred with naïve OT-II cells (OT-II→WT and OT-II→$Cd3e^{-/-}$) were immunized with (A) OVA in alum, (B) OVA+MPL, or (C–F) NP_{19}-OVA in alum. (A) The number of endogenous GC B cells (left, 7-AAD⁻CD19⁺B220⁺FAS⁺GL-7⁺) and plasma cells (right, 7-AAD⁻CD19$^{int/low}$CD138⁺) in the spleen at the indicated time points was determined by flow cytometry. (B) Fixed spleen cryosections obtained at the indicated time points after immunization and stained with anti-IgD (naïve B cells), anti-CD45.1 (OT-II cells), and GL-7 (GC B cells). Original magnification: 15×. (C) The kinetics of total (binding to NP_{23}-BSA) and high-affinity (binding to NP_3-BSA) NP-specific IgG1 serum antibody levels were determined by ELISA. (D) The ratio between high-affinity and total NP-specific IgG1 antibodies as a relative measure of affinity maturation is shown (E and F). The number of (E) NP-specific total and high-affinity IgG1⁺ antibody-secreting cells (ASCs) and of (F) total IgG1⁺ ASCs in spleen and bone marrow on day +25 after immunization was determined by ELISPOT. Data shown are mean ± SEM (n = 2–6) and experiment representative of at least three independent experiments performed. Significance analyzed by nonparametric unpaired Mann-Whitney U test. *$p < 0.05$; **$p < 0.01$. Where not indicated, the p values were not significant.

provide bystander help to B cells of unrelated specificities, including autoreactive B cells [8].

Taken together, these findings indicate that the exuberant monoclonal Tfh-cell response in OT-II→$Cd3e^{-/-}$ mice impairs the ability of these cells to induce affinity maturation of antigen-stimulated B cells, generation of high-affinity antibodies and of long-lived plasma cells.

Altered distribution of antigen-specific B cells in the GCs of OT-II→$Cd3e^{-/-}$ mice

The movement of GC B cells between anatomically distinct LZ and DZ areas is critical for the selection process of mutated B-cell clones [4]. To define the distribution of polyclonal and NP-specific B cells within the GCs of OT-II→WT and OT-II→$Cd3e^{-/-}$ mice, we
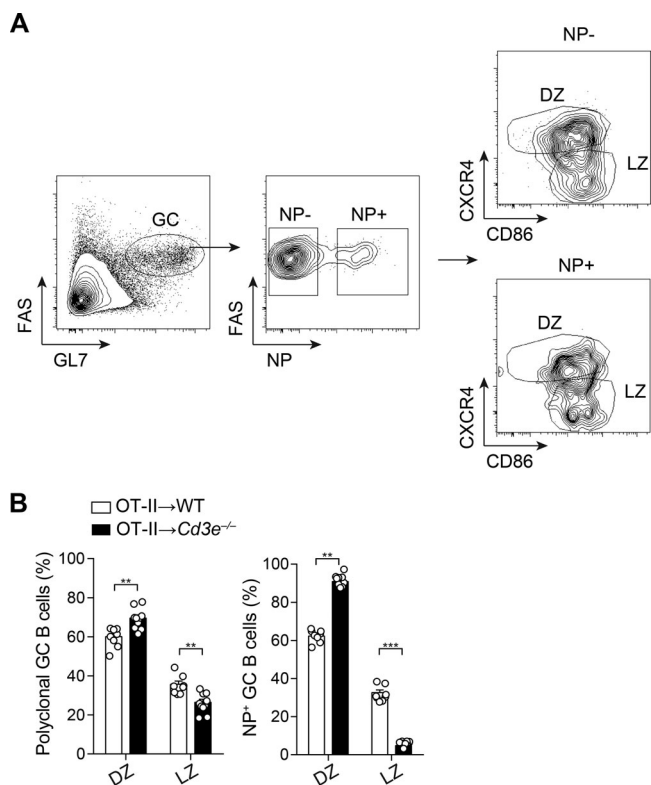
A

B

Figure 2. Altered GC B-cell distribution within dark and light zone in $Cd3e^{-/-}$ mice. (A) Contour plots of a representative staining of CD19$^+$B220$^+$ splenic B cells on day +10 after i.p. immunization of OT-II→WT mice with NP-OVA. After gating on GL7$^+$ FAS$^+$ GC B cells (left), NP$^-$ and NP$^+$ (middle) cells are identified, and a representative dark zone (DZ, CXCR4^{hi}CD86^{lo}) and light zone (LZ, CXCR4^{lo}CD86^{hi}) gating strategy is shown (right). (B) The percentage of polyclonal (left) and NP-specific (right) DZ and LZ GC B cells in OT-II→WT and OT-II→$Cd3e^{-/-}$ mice was determined by flow cytometry. Data shown are mean ± SEM (n = 8–10) and representative of at least two independent experiments performed. Significance analyzed by nonparametric unpaired Mann-Whitney U test. **p < 0.01; ***p < 0.001. Where not indicated, the p values were not significant.

stained polyclonal (NP$^-$) and NP-specific B cells (NP$^+$) with antibodies to CXCR4 and CD86, which can be used to distinguish LZ and DZ cells [13] (Fig. 2A). In WT recipients, a high proportion of polyclonal and NP-specific B cells displayed a CXCR4$^-$CD86$^+$ phenotype, indicating that in these mice there was an increased localization of these cells in the LZ (Fig. 2B). In contrast, in $Cd3e^{-/-}$ recipients, both B-cell populations were mainly CXCR4$^+$CD86$^-$, consistent with their preferential localization and expansion in the DZ. In particular, NP-specific GC B cells were almost entirely confined in the DZ, with the percentage of GC B cells in the LZ of $Cd3e^{-/-}$ mice being significantly lower as compared to the percentage of NP-specific GC B cells in the LZ of WT mice (Fig. 2B).

To more precisely follow the fate of antigen-specific B cells in our experimental system, we co-transferred CD45.1 SW$_{HEL}$ transgenic B cells [14], which express a monoclonal BCR (HyHEL10) that recognizes hen egg lysozyme (HEL), into OT-II→$Cd3e^{-/-}$ or OT-II→WT mice (Fig. 3A). Recipient mice were then immunized with a HEL^{wt}-OVA$_{323-339}$ fusion protein in order to promote the

cognate interaction between SW$_{HEL}$ B cells and OT-II T cells [14]. HEL-specific and endogenous polyclonal B cells were analyzed on day +7 and day +19 after immunization. As shown in Figure 3B, expansion of SW$_{HEL}$ B cells was greater in $Cd3e^{-/-}$ mice than in WT mice. However, in $Cd3e^{-/-}$ mice, only a small fraction of SW$_{HEL}$ B cells differentiated into GC B cells as compared to SW$_{HEL}$ B cells in WT mice, both at early (39.3% ± 2.7% vs 68.4% ± 5.3%) and late (2.1% ± 0.7% vs 69.6% ± 11.1%) time points (Fig. 3C and D). In addition, SW$_{HEL}$ GC B cells in $Cd3e^{-/-}$ mice expressed lower levels of AID mRNA as compared to GC B cells in WT mice (Fig. 3E), suggesting a reduced rate of somatic mutation of immunoglobulin variable genes during the GC reaction. In contrast, in $Cd3e^{-/-}$ mice a large fraction of splenic SW$_{HEL}$ B cells differentiated into short-lived plasma cells (Fig. 3F and G), consistent with the finding that CD138$^+$ cells were present in extrafollicular regions of the spleen, outside of the CD35$^+$ GC area (Supporting Information Fig. S3).

Taken together, these data demonstrate that high numbers of Tfh cells impair GC dynamics and the generation of antigen-specific GC B cells.

Pre-reconstitution of $Cd3e^{-/-}$ mice with Treg cells restores GC B-cell dynamics and affinity maturation

Follicular regulatory T (Tfr) cells have been previously implicated in the control of the GC reaction [15–18]. To explore the role of Treg cells in our experimental system, $Cd3e^{-/-}$ mice were adoptively transferred with CD4$^+$CD25^{hi} (GFP$^+$) Treg cells from Foxp3/GFP$^+$ transgenic reporter mice, 2–3 weeks before receiving naïve OT-II cells and SW$_{HEL}$ B cells (Fig. 4A). Different groups of mice were then immunized with HEL-OVA and analyzed on day +9. In line with previous reports [19, 20], we observed that a small fraction (~20%) of the transferred Foxp3/GFP$^+$ Treg cells lost Foxp3 expression in $Cd3e^{-/-}$ mice, while 4.5% (range 1.2–10.8%) of Foxp3/GFP$^+$ cells acquired a ICOS$^+$/PD1$^+$ CXCR5$^+$ Tfr-cell phenotype, expressing high levels of CD25 and CTLA-4 (Supporting Information Fig. S4A–C), as indication of their suppressive ability [21].

Strikingly, in immunized OT-II→$Cd3e^{-/-}$ mice reconstituted with Treg cells, the expansion of OT-II cells and their differentiation into Tfh cells was drastically reduced, reaching levels that were comparable to those measured in WT recipients (Fig. 4B). In these mice, there was also a significant reduction in the numbers of total and GC SW$_{HEL}$ B cells as compared to OT-II→$Cd3e^{-/-}$ mice, reaching also in this case levels that were comparable to those measured in OT-II→WT mice (Fig. 4C). Importantly, a significantly higher frequency of GC SW$_{HEL}$ B cells in Treg-$Cd3e^{-/-}$ recipients acquired a phenotype indicative of their preferential localization in the GC LZ, resembling the same distribution observed in WT mice (Fig. 4D). Finally, the frequency and number of antigen-specific plasma cells in spleen were reduced in Treg-$Cd3e^{-/-}$ recipients as compared to $Cd3e^{-/-}$ recipients (Fig. 4E). Thus, Treg cells were able to limit the exuberant Tfh response and the altered GC B-cell dynamics observed in lymphopenic $Cd3e^{-/-}$ recipients.
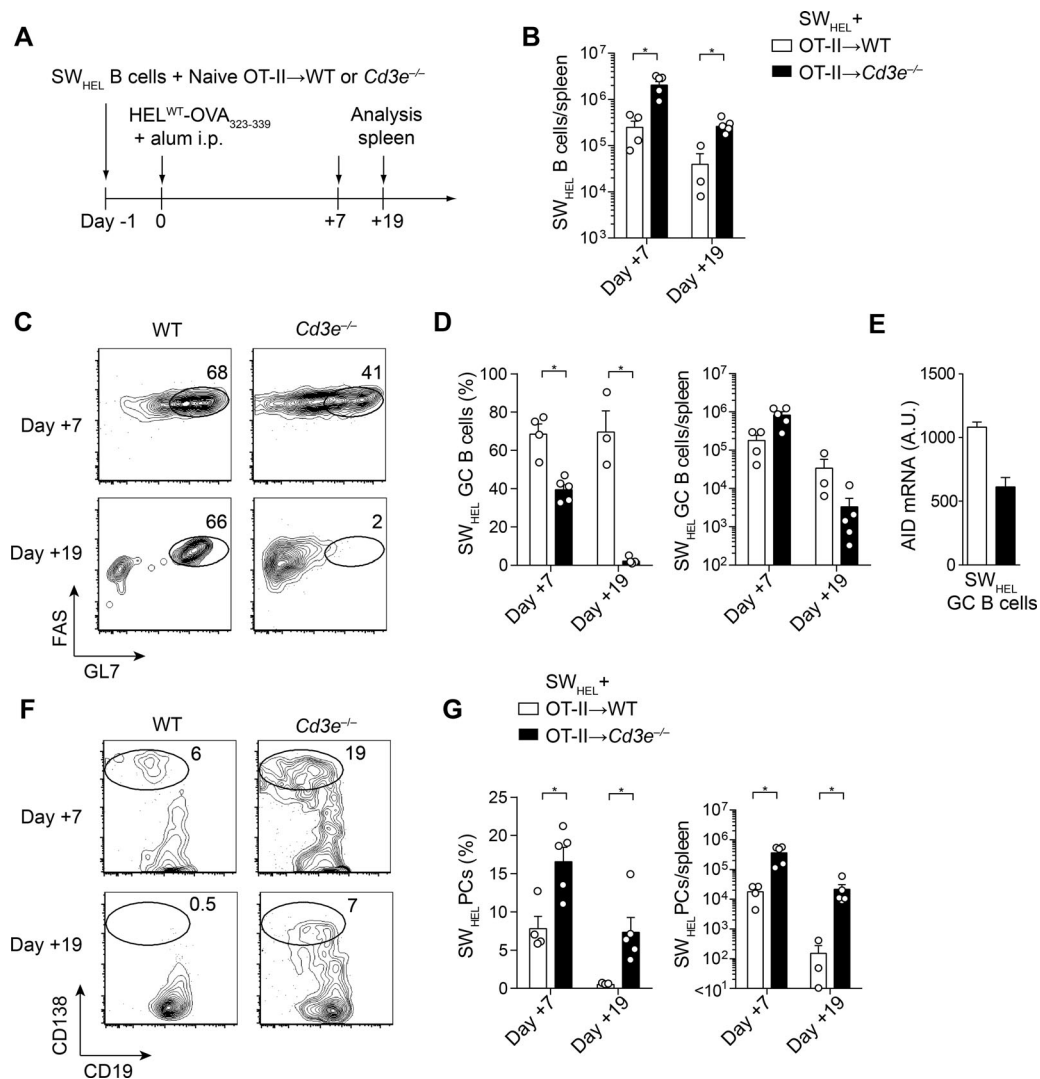
Figure 3. In the presence of high numbers of Tfh cells, antigen-activated B cells give rise to few GC B cells expressing low levels of AID. (A) Schematic outline of the experimental approach. (B) The numbers of splenic SW$_{HEL}$ B cells (7-AAD$^-$CD45.1$^+$CD19$^+$B220$^+$) at the indicated time points in OT-II→WT and OT-II→$Cd3e^{-/-}$ mice cotransferred with SW$_{HEL}$ cells were quantified by flow cytometry. (C) Representative dot plots showing expression of GL-7 and FAS on 7-AAD$^-$CD45.1$^+$CD19$^+$B220$^+$ splenic cells. Numbers indicate percentages of cells within the indicated gates. (D) The percentages and absolute numbers (mean ± SEM) of SW$_{HEL}$ GC B cells as determined in (C) are shown. (E) AID mRNA expression levels (expressed as A.U.) were assessed in SW$_{HEL}$ GC B cells isolated from OT-II→WT and OT-II→$Cd3e^{-/-}$ mice cotransferred with SW$_{HEL}$ cells (day+23 days post immunization with HEL-OVA). (F) Representative dot plots showing expression of CD19 and CD138 on splenic plasma cells (PCs) on 7-AAD$^-$CD45.1$^+$ cells. Numbers indicate percentages of cells in the indicated gate. (G) The percentages and absolute numbers (mean ± SEM) of SW$_{HEL}$ PCs determined as in (F) are shown. Data shown were obtained with n = 4 (WT) and n = 5 ($Cd3e^{-/-}$), and are representative of at least four independent experiments performed. Significance was determined by the nonparametric unpaired Mann-Whitney U test. $^*p < 0.05$. Where not indicated, the p values were not significant.

We also tested the ability of Treg cells to re-establish affinity maturation of the anti-NP B-cell response upon immunization with NP-OVA performed as described in Figure 1. As in the case of immunization with HEL-OVA, Tfh-cell and GC B-cell numbers in Treg-reconstituted $Cd3e^{-/-}$ mice returned to levels comparable to those of WT mice (data not shown). Furthermore, high-affinity anti-NP$_3$ antibodies and the ratio of anti-NP$_3$/anti-NP$_{23}$ antibodies increased in Treg-$Cd3e^{-/-}$ mice (Supporting Information Fig. S5A and B). Moreover, the elevated serum IgE level, which is a hallmark of the polyclonal B-cell activation occurring in $Cd3e^{-/-}$ mice after expansion of Tfh cells [8], was also reduced when

mice were reconstituted with Treg cells (Supporting Information Fig. S5C).

Limited SHM of SW$_{HEL}$ B cells in OT-II→$Cd3e^{-/-}$ mice

To further analyze the quality of the GC reaction, we sequenced the variable heavy chain (V$_H$10) gene of individual HEL-specific GC SW$_{HEL}$ B cells isolated from the different groups of mice and aligned them to the original targeting construct used to generate SW$_{HEL}$ mice [22]. In this set of experiments, mice were immunized with HEL^{2X}-OVA, which binds with lower affinity to the
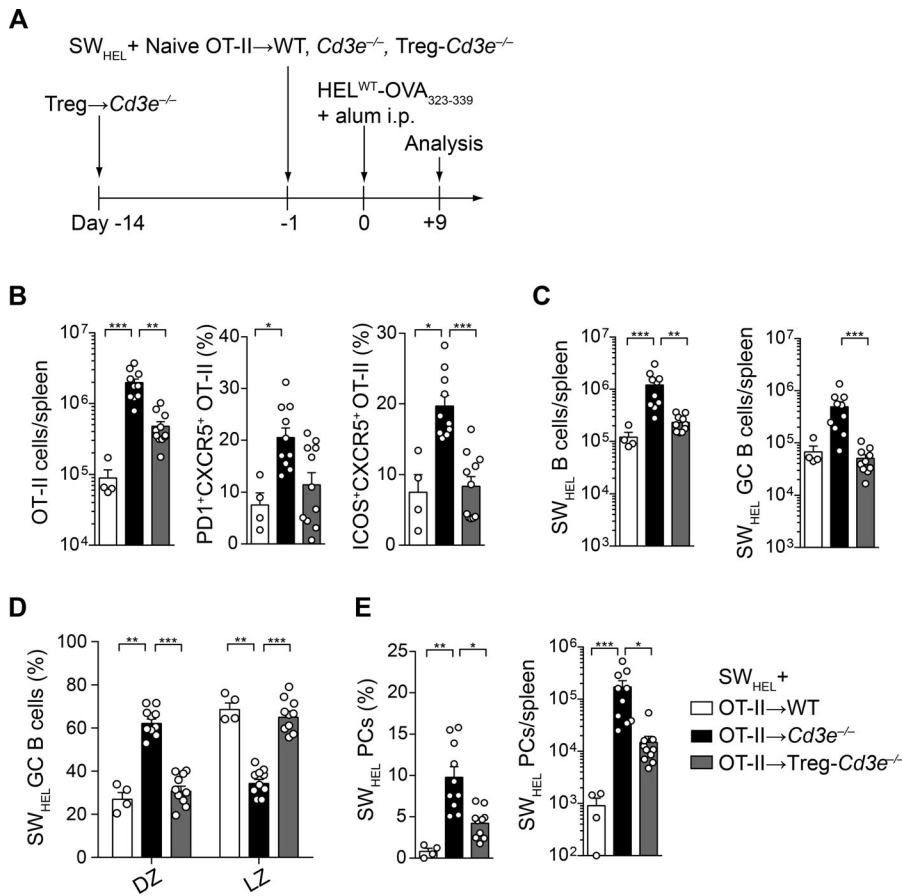
Figure 4. Treg cells limit Tfh-cell numbers and change the fate of antigen-activated B cells. (A) Schematic outline of the experimental approach. (B) OT-II-cell numbers (7-AAD$^-$GFP^{hi}CD4$^+$, left) and percentage of OT-II Tfh cells (CXCR5$^+$PD1$^+$ and CXCR5$^+$ICOS$^+$, right) in the spleens of SW$_{HEL}$- and OT-II-adoptively transferred WT mice, $Cd3e^{-/-}$ mice, or $Cd3e^{-/-}$ mice that had received CD4$^+$Foxp3/GFP$^+$ T cells (Treg→$Cd3e^{-/-}$) 14 days before. (C) Numbers of total SW$_{HEL}$ B cells (7AAD$^-$CD19$^+$B220$^+$CD45.1$^+$) and GC SW$_{HEL}$ B cells (7AAD$^-$CD19$^+$B220$^+$CD45.1$^+$GL-7$^+$FAS$^+$) in the spleens of the three groups of mice. (D) Percentage of dark zone (DZ, CD19$^+$B220$^+$FAS$^+$GL-7$^+$CXCR4^{hi}CD86^{lo}) and light zone (LZ, CD19$^+$B220$^+$FAS$^+$GL-7$^+$CXCR4^{lo}CD86^{hi}) GC B cells within SW$_{HEL}$ GC B cells. (E) Percentage and numbers of HEL-specific splenic PCs (7-AAD$^-$CD45.1$^+$CD19$^{int/lo}$CD138$^+$). Cell numbers and percentages were determined by flow cytometry. Data shown are mean ± SEM (n = 4–11) and representative of at least three independent experiments performed. Significance was determined by the nonparametric Kruskal-Wallis test followed by Dunn's post hoc test. $^*p < 0.05$; $^{**}p < 0.01$; $^{***}p < 0.001$. Where not indicated, the p values were not significant.

SW$_{HEL}$ BCR, in order to promote the induction of SHM. At an early time point (day +10), mutation frequencies of nucleotides (Supporting Information Fig. S6) and amino acids (Fig. 5) were comparable between GC B cells isolated from OT-II→WT, OT-II→$Cd3e^{-/-}$, and OT-II→Treg-$Cd3e^{-/-}$ mice. In contrast, at late time points (around three weeks after immunization), GC B cells isolated from WT and Treg-$Cd3e^{-/-}$ mice showed higher numbers of nucleotide and amino acid substitutions as compared to B cells isolated from $Cd3e^{-/-}$ mice that had not received Treg cells (Fig. 5 and Supporting Information Fig. S6).
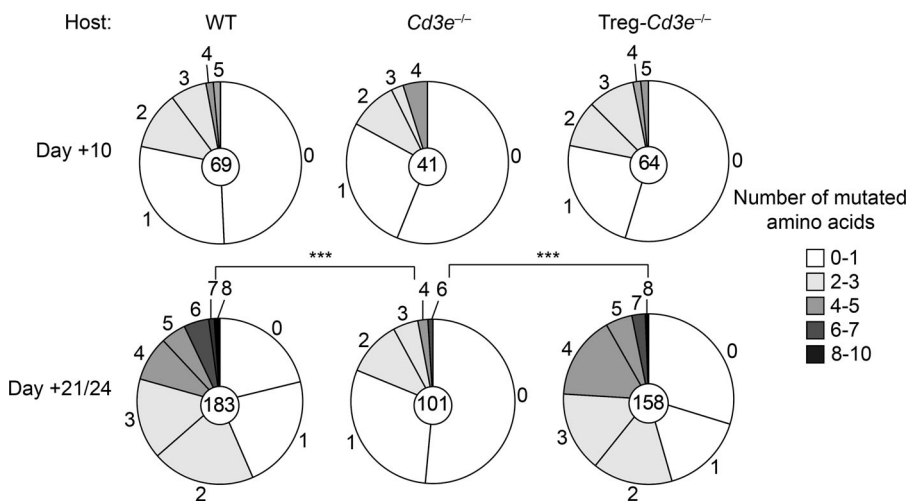

Figure 5. High numbers of Tfh cells limit somatic mutation, which is restored by the addition of Treg cells. In an experimental set-up as described in Figure 4A, the three groups of mice were immunized i.p. with HEL^{2x}-OVA$_{323-339}$ in alum. On day +10 and or +21/24, several single SW$_{HEL}$ GC B cells (7-AAD$^-$ CD45.1$^+$CD19$^+$B220$^+$IgD$^-$IgM$^-$GL-7$^+$FAS$^+$) were sorted from one mouse of each group and cDNA was prepared for immunoglobulin gene sequencing. Pie charts display the numbers of amino acid mutations at early (top, day +10) and late time points (bottom, day +21/24). Circle segments are proportional to the number of sequences with the indicated number of amino acid substitutions. Total numbers of analyzed sequences are indicated in the center of each pie chart. Data are pooled from three independent experiments performed (each with 1–3 mice analyzed). Significance was determined by the nonparametric Kruskal-Wallis test followed by Dunn's post hoc test. $^{***}p < 0.001$. Where not indicated, the p values were not significant.
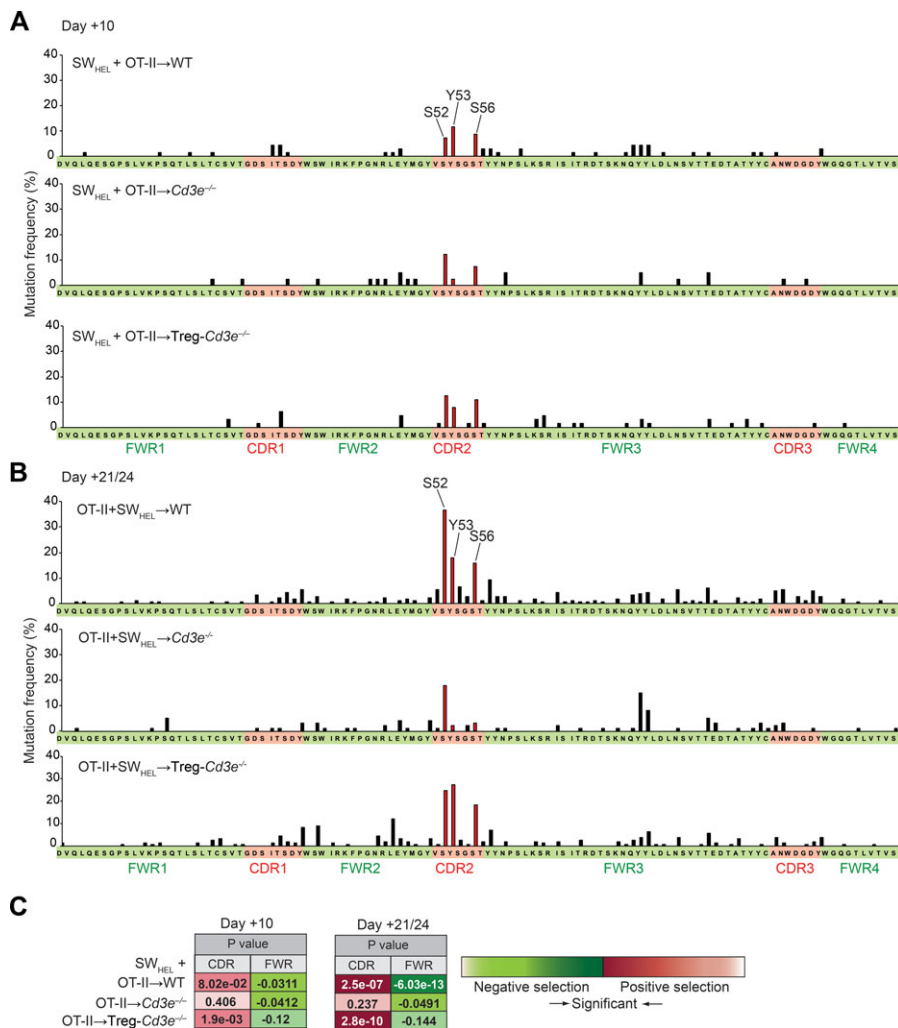
Figure 6. Positive selection of SW$_{HEL}$ B-cell clones in WT and $Cd3e^{-/-}$ mice reconstituted with Treg cells. (A and B) The V$_H$10 amino acid sequence (with the indicated FWRs and CDRs regions) is indicated on the x axis and the mutation frequencies among all clones are displayed on the y axis for OT-II+SW$_{HEL}$→WT, OT-II+SW$_{HEL}$→$Cd3e^{-/-}$, and OT-II+SW$_{HEL}$→Treg-$Cd3e^{-/-}$ mice on (A) day +10 and (B) day +21/24. The red peaks within the CDR2 are important binding residues for HEL. (C) The indicated p values for the FWRs and CDRs were obtained with the Bayesian estimation of antigen-driven selection in immunoglobulin sequences for both day +10 (left) and day +21/24 (right) for the three groups of mice. The red and green colors are associated with positive and negative selection of B-cell clones respectively, with light and dark colours indicating nonsignificant ($p > 0.05$) and significant ($p \leq 0.05$) selection, respectively. p-values less than zero indicate negative selection. Data are pooled from three independent experiments performed (each with 1–3 mice analyzed).

When all VH sequences were aligned, we observed that at early time points, the positions of the mutated amino acids were comparable between HEL-specific GC B cells isolated from the three groups of mice (Fig. 6A). However, at late time points, B-cell clones from WT and Treg-$Cd3e^{-/-}$ groups displayed mutations mostly within the CDR regions, particularly in the CDR2. Moreover, certain amino acid residues present in the CDR2 (S52, Y53, S56, peaks colored in red), previously reported to be crucial for high-affinity binding to HEL [23–25], were found to be highly mutated in clones isolated from WT and Treg-$Cd3e^{-/-}$ mice, but much less in clones from $Cd3e^{-/-}$ mice (Fig. 6B).

To understand the driving force of selection of the analyzed sequences, we used the Bayesian estimation of Tfh/antigen-driven selection in immunoglobulin sequences [26, 27]. From such algorithm, we obtained the indicated p values for the FWRs and CDRs of the three groups of mice (Fig. 6C). At early time points, all B-cell clones showed negative selection for the FWR regions and weak positive selection for the CDR regions, however, with higher significance for clones isolated from WT and Treg-$Cd3e^{-/-}$ mice as compared to those derived from $Cd3e^{-/-}$ mice. At late time points, a very low positive p value was associated with the CDR regions of WT and Treg-$Cd3e^{-/-}$ sequences, indicating strong positive, antigen/Tfh-driven, selection of the isolated clones, whereas FWR regions were associated with negative selection. In contrast, HEL-specific GC B-cell clones from $Cd3e^{-/-}$ mice displayed similar p values observed at the early time point for both FWRs and CDRs, implicating a random, non-Tfh-cell selected accumulation of mutations (Fig. 6C).

Overall, these somatic mutation data underline the role of Tfh-cell numbers in the selection of high-affinity B-cell clones, resulting in the generation of low-affinity antigen-specific antibodies in the presence of high numbers of Tfh cells. Of note, Treg cells, most likely by restraining the numbers of Tfh cells, were able to restore the selection of mutated antigen-specific B-cell clones within the GC LZ.

CXCR5-deficient Treg cells and non-regulatory memory CD4$^+$ T cells can control the GC reaction

Previous studies have demonstrated that CXCR5 plays a crucial role in Tfr-cell function, since it drives migration of these cells into the B-cell follicle where they exert their suppressive function on GB B and Tfh cells [15–17, 28]. To assess in our experimental
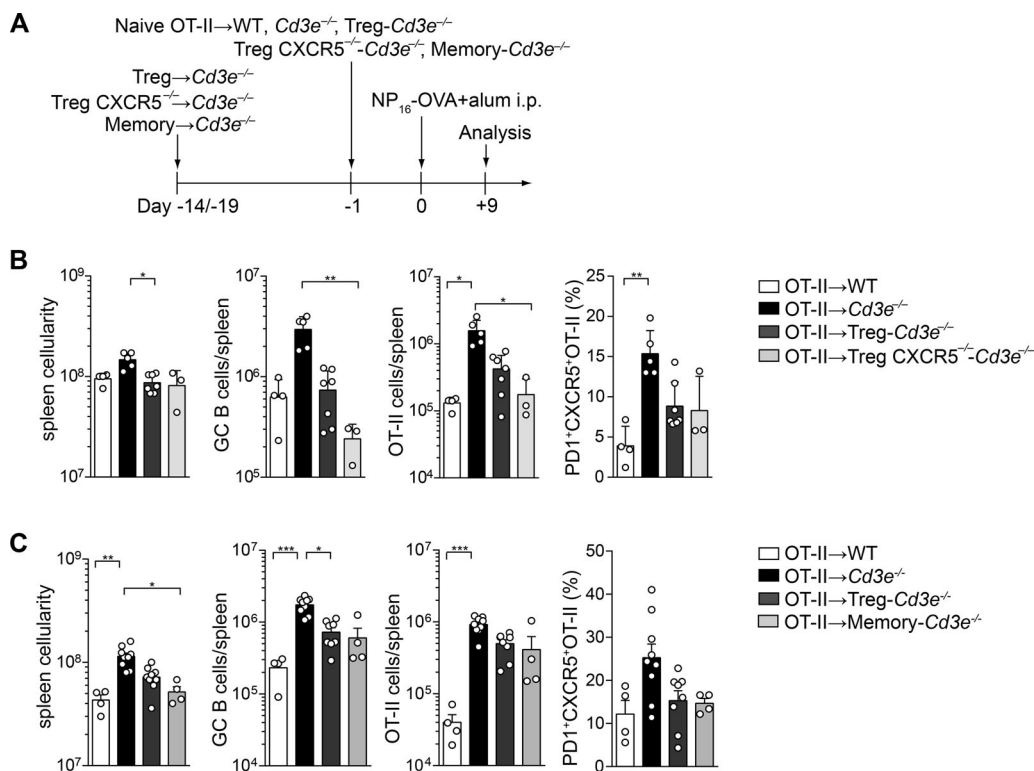
Figure 7. CXCR5$^{-/-}$ Treg cells and CXCR5$^{+/+}$ memory T cells limit the GC reaction to the same degree as WT Treg cells. (A) Schematic outline of the experimental approach. (B) Treg cells (CD4$^+$CD8$^-$CD25^{high}) were isolated from WT or CXCR5$^{-/-}$ mice, and (C) Foxp3/GFP$^+$ Treg cells or Foxp3/GFP$^-$ memory T cells were isolated from Foxp3/GFP$^+$ transgenic mice, transferred to $Cd3e^{-/-}$ hosts, and allowed to homeostatically expand for (B) 14 days or (C) 19 days. Then, WT, $Cd3e^{-/-}$, Treg-$Cd3e^{-/-}$, CXCR5$^{-/-}$Treg-$Cd3e^{-/-}$, and memory-$Cd3e^{-/-}$ hosts received OT-II cells i.v. and were immunized i.p. with NP$_{16}$-OVA in alum. (B and C) Mice were sacrificed on day +9 and the following cellular parameters were analyzed: spleen cellularity, GC B-cell numbers (7AAD$^-$CD19$^+$B220$^+$FAS$^+$GL-7$^+$), OT-II-cell numbers (7-AAD$^-$CD45.1$^+$CD4$^+$), and percentage of OT-II expressing Tfh-cell markers (PD1$^+$CXCR5$^+$) were determined by flow cytometry. Data shown are mean ± SEM (n = 4–8) and representative of at least three independent experiments performed. In $Cd3e^{-/-}$ hosts, CXCR5-sufficient and CXCR5-deficient Treg cells reached similar expansion and expressed comparable high levels of CD25 (data not shown). Significance was determined by the nonparametric Kruskal-Wallis test followed by Dunn's post hoc test. $^*p < 0.05$; $^{**}p < 0.01$, $^{***}p < 0.001$. Where not indicated, the p values were not significant.

system the role of Treg cells outside of the B-cell follicles and the role of non-regulatory T cells, we reconstituted $Cd3e^{-/-}$ mice with CXCR5-sufficient or CXCR5-deficient Treg cells or with non-regulatory Foxp3$^-$ CD44^{hi} memory CD4$^+$ T cells (Fig. 7A). Treg cells and memory T cells were allowed to expand homeostatically for 14–19 days; successively, mice received naïve OT-II cells and were immunized with NP$_{16}$-OVA in alum. Strikingly, in comparison to $Cd3e^{-/-}$ mice that only received OT-II cells, both CXCR5-sufficient and CXCR5-deficient Treg cells as well as memory CD4$^+$ T cells were able to reduce spleen cellularity and GC B-cell and OT-II-cell expansion. Moreover, the percentage of OT-II cells that acquired Tfh-cell markers was reduced (Fig. 7B and C).

Taken together these results suggest that cognate interactions between Tfh and GC B cells can be controlled by Treg and Tfr cells both in the T-cell area and in the B-cell follicle, through mechanisms that may involve competition for available IL-2 and signals through inhibitory receptors, such as CTLA-4. They also suggest that other types of competing non-regulatory T cells may act through similar or different mechanisms in order to control the GC reaction.

Discussion

In this study, we characterized the response of adoptively transferred HEL-specific and endogenous NP-specific B cells in lymphopenic $Cd3e^{-/-}$ mice adoptively transferred with monoclonal OT-II transgenic T cells. Our results suggest a lack of selection of high-affinity B-cell clones in $Cd3e^{-/-}$ mice in the presence of high numbers of Tfh cells. Antigen-specific B cells received sufficient signals from Tfh cells to migrate toward the DZ of GCs in $Cd3e^{-/-}$ mice, suggesting that they could potentially accumulate mutations. As a matter of fact, at the beginning of the GC reaction (around day +10) the affinity of the antibody response and the somatic mutation rates were comparable in the presence of normal or high numbers of Tfh cells (in WT and $Cd3e^{-/-}$ hosts, respectively). However, over time a sustained GC reaction in $Cd3e^{-/-}$ mice led to the lack of selection of B-cell clones by Tfh cells in the LZ, which did not allow for survival of high-affinity B-cell clones. In WT mice, small and controlled numbers of Tfh cells provided survival signals mostly to high-affinity B cells that were more efficient in binding and presenting peptide-MHC-II complexes to

T cells. The result of this positive selection was the generation of high-affinity antibodies in the sera of immunized OT-II→WT mice. Moreover, the somatic mutation pattern in WT mice was consistent with Tfh-driven positive selection, because of the preferential accumulation of replacement mutations within the CDR rather than within the FWR regions [29]. In OT-II→*Cd3e*−/− mice, high numbers of Tfh cells provided help to B cells with a wide range of affinities and specificities [8]. The consequence of this indiscriminate provision of help was the lack of selection of high-affinity B cells.

Recently, Tfr cells able to control the GC reaction have been described [15–17]. However, the contribution of Tfr and Treg cells on the selection of GC B-cell clones remained unclear. In accordance with these recent findings, we showed that pre-reconstitution of *Cd3e*-deficient mice with Treg cells restrained the expansion of Tfh cells and GC B cells. Moreover, we found that the transfer of Treg cells drove the distribution of both polyclonal and antigen-specific GC B cells within the LZ, which was sufficient to restore the generation of high-affinity antibodies. Importantly, the accumulation of mutations critical for the high-affinity binding of the transgenic HyHEL10 BCR to the antigen was restored in the presence of Treg cells, in a comparable manner to WT recipients. Since there is a tight correlation between Tfh and GC B-cell numbers [8], it is difficult to test if Treg cells and Tfr cells act directly on Tfh cells and/or on GC B cells. In our opinion, Tfr cells could function by reducing the numbers of Tfh cells, which would result in reduced signals to LZ GC B cells to migrate toward and accumulate in the DZ. Through the data obtained with CXCR5-deficient Treg cells, we suggest a crucial role for both Treg and Tfr cells in the control of the GC reaction, which is in contrast to recent reports that highlighted the exclusive role of Tfr cells in the suppression of Tfh and GC B-cell differentiation both in WT and lymphopenic mice [15–17]. This discrepancy is most likely due to different experimental settings, in particular the pre-transfer and expansion of Treg cells in lymphopenic *Cd3e*−/− mice reduced the empty space and the driving force of OT-II-cell proliferation, and consequently of GC B-cell and Tfh-cell differentiation. As a matter of fact, we obtained similar control of the GC reaction through the pre-transfer of non-regulatory memory T cells, that also reduce the empty space in *Cd3e*-deficient mice.

The findings reported in this work may be relevant for the management of patients with lymphopenia [30], defects in lymphocyte homeostasis, or HIV-1 infection [31]. Notably, a crucial association between chronic HIV-1 infection, dysregulated Tfh cells and lack of neutralizing antibodies has been recently described [31]. Moreover, other chronic infections have also been associated with exaggerated Tfh-cell expansion, such as *Salmonella* [32] and lymphocytic choriomeningitis infection [33].

In summary, we showed that high numbers of Tfh cells lead to defective antigen-specific B-cell responses, characterized by a lack of high-affinity antibodies and high-affinity long-lived plasma cells. Reconstitution of *Cd3e*−/−hosts with Treg cells was sufficient to reduce the numbers of Tfh and GC B cells as well as to restore the distribution of GC B cells in the LZ and therefore the selection of high-affinity B-cell clones. Moreover, in these conditions,

we reported for the first time the anatomical distribution of GC B cells between the DZ and the LZ and the molecular analysis of the antibody response in terms of somatic mutations in the absence or presence of Treg cells. Our study suggests that if crucial checkpoints that regulate Tfh-cell numbers and function are missing, such as in the context of infection or vaccination, antibodies with autoreactive properties can arise at the expense of protective high-affinity antigen-specific antibodies.

Materials and methods

Mice

Cd3e−/− [9] and SW_HEL (kindly provided by Robert Brink, Garvan Institute, Ref. [14]) mice have been described previously. OT-II (004194), Foxp3/GFP (006772), and *Cxcr5*−/− (006659) mice were obtained from The Jackson Laboratory. C57BL/6 (wild-type, WT) mice were obtained from Harlan Italy Srl. All TCR- and BCR-transgenic mouse strains, including OT-II and SW_HEL, were bred and maintained on a *Rag1*−/− background. In order to identify transferred cells within hosts, donor mice were bred onto homo- or heterozygous CD45.1 allele or UBC-GFP (004353) backgrounds. All mice were bred and maintained under specific pathogen-free conditions. Animals were treated in accordance with the guidelines of the Swiss Federal Veterinary Office. Experiments were approved by the Dipartimento della Sanità e Socialità of Canton Ticino.

Adoptive cell transfers

Spleens and peripheral lymph nodes were minced between the frosted ends of microscope glass slides to obtain single-cell suspensions that were then filtered through fine mesh. Naïve CD4$^+$CD8$^-$CD44^{lo}CD62L^{hi}CD25$^-$ T cells were first enriched with anti-CD4 microbeads (L3T4) (Miltenyi Biotec) and then sorted on a FACSAria cell sorter (BD Biosciences) to >99% purity. Low numbers of T cells (3–5 × 10^4 cells per mouse) were injected intravenously (i.v.) and cells were allowed to equilibrate within the host for 16–24 h before immunization. HEL-specific B cells were obtained from SW_HEL mice using anti-CD43 antibody-conjugated microbeads (Ly-48) (Miltenyi Biotec). For adoptive co-transfer of HEL-specific B cells and OVA-specific T cells, recipient mice were injected i.v. with 3–5 × 10^4 SW_HEL B cells and 3–5 × 10^4 naïve OT-II cells. Treg cells and memory T cells, isolated from Foxp3/GFP mice that carried one CD45.1 allele (CD45.1/2), were first pre-enriched with anti-CD4 microbeads and then sorted on a FACSAria cell sorter as CD4$^+$CD8$^-$GFP$^+$CD25^{hi} and CD4$^+$CD8$^-$CD44^{hi}GFP$^-$CD25$^-$ cells, respectively. Alternatively, Treg cells were isolated from WT or *Cxcr5*−/− mice, pre-enriched with anti-CD4 microbeads, and then sorted on a FACSAria cell sorter as CD4$^+$CD8$^-$CD25^{hi} cells. *Cd3e*−/− mice were injected i.v. with 1×10^5 Treg or memory T cells. OT-II

cells that carried a UBC-GFP transgene were identified as GFP^{hi} cells, whereas Treg cells were GFP^{dim}.

Antigens and immunizations

Mice were immunized intraperitoneally (i.p.) with 50 μg endotoxin-free ovalbumin (Endograde OVA; Profos) in combination with monophosphoryl lipid A (Sigma-Aldrich) or Imject alum (Thermo Scientific) as adjuvants. For analysis of affinity maturation, OT-II-cell transferred WT or $Cd3e^{-/-}$ mice were immunized i.p. with 50 μg NP$_{19}$-OVA (Biosearch Technologies) in alum. For SW$_{HEL}$ and OT-II co-transfers, mice were immunized i.p. with 30–35 μg of HEL^{WT}-OVA$_{323-339}$ or the mutated form HEL^{2X}-OVA$_{323-339}$ in alum (recombinant proteins were kindly provided by Humabs BioMed).

Flow cytometry

The following antibodies or streptavidin, conjugated to biotin, FITC, Alexa Fluor (AF) 488, AF647, PE, PE-Cy7, PerCP-Cy5.5, APC, APC-Cy7, Pacific Blue, Pacific Orange, BV605 or BV785, were purchased from BD Biosciences, eBioscience, Biolegend, or Molecular Probes: CD3ε (clone: 145-2C11), CD4 (RM4-5), CD8 (53-6.7), CD19 (1D3), CD25 (7D4), CD62L (MEL-14), CD44 (IM7), CD45.1 (A20), CD45.2 (104), CD86 (GL-1), CD127 (A7R34), PD-1 (RMP1-30), B220 (RA3-6B2), FAS (Jo2), GL-7, CXCR5 (2G8), PSGL-1 (2PH-1), CXCR4 (12G5), CD21 (7E9), CD23 (B3B4), ICOS (7E.17G9), CD69 (H1.2F3), BTLA (8F4), CD138 (281-2), IgM (R6-60.2), IgD (11-26c-2a), IFN-γ (XMG1.2), IL-4 (11B11), IL-17A (TC11-18H10.1), Bcl-6 (K112-91), Foxp3 (FJK-16s), CTLA-4 (UC10-4B9). Intracellular staining of Bcl-6, Foxp3 and CTLA-4 has been performed using the Foxp3-staining buffer set from eBioscience (00-5523). NP$_{40}$-PE was purchased from Biosearch Technologies. Intracellular staining for IL-21 was performed using recombinant mouse IL-21R-Fc Chimera (R&D) and secondary R-Phyco affinity pure R(ab')2 fragment goat anti-human IgG, Fcγ Frag Spec (Jackson Laboratories). Flow cytometry was performed on a FACSCanto II or LSRFortessa (BD Biosciences) and data was evaluated using FlowJo software (TriStar).

ELISA/ELISPOT

ELISA was performed as previously described [8]. To determine antigen-specific antibodies, 96-well ELISA plates were coated with NP$_{23}$-BSA or NP$_3$-BSA in PBS (10 μg/mL). The ratio between NP$_3$-versus NP$_{23}$-binding antibodies was calculated as an estimate for affinity maturation. Arbitrary units of antigen-specific antibodies were calculated according to reference serum from NP$_{19}$-OVA hyper-immunized mice. IgE levels were determined as previously described [8]. For intracellular cytokine (ICC) staining, CD45.1$^+$ OT-II T cells were enriched by MACS and further sorted by flow cytometry as CD45.1$^+$CD4$^+$CXCR5$^+$ or CD45.1$^+$CD4$^+$CXCR5$^-$

cells. For ICC staining, cells were stimulated for 5 h with 1 nM phorbol 12-myristate 13-acetate (PMA, Sigma) and 1 μg/mL ionomycin (Sigma) with the last 3 h in the presence of Brefeldin A (10 μg/mL; Sigma). Cells were fixed in 4% (wt/vol) paraformaldehyde and permeabilized with 0.5% (wt/vol) saponin (Sigma-Aldrich). For ELISPOT, single-cell suspensions of spleen and BM were counted and $1 \times 10^5 - 1 \times 10^6$ cells were applied to the top wells of a regular 96-well plate, titrated, and subsequently transferred to pre-blocked ELISPOT plates. Cells were incubated overnight and ASCs were detected with biotin-conjugated anti-Ig antibodies (Southern Biotech), followed by avidin-HRP (Sigma-Aldrich). Spots were visualized using AEC tablets (Sigma-Aldrich) and counted under a stereo microscope (Zeiss).

SHM analysis

WT, $Cd3e^{-/-}$ and Treg-$Cd3e^{-/-}$ mice received $3–5 \times 10^4$ naïve OT-II cells (UBC-GFP$^+$ or CD45.1/2+) and $3–5 \times 10^4$ SW$_{HEL}$ B cells (UBC-GFP+ or CD45.1$^+$). Mice were immunized i.p. with 30–35 μg HEL^{2X}-OVA in alum. Mice were sacrificed on day +10 or day +21/24 (according to the different experiments) and spleens were dissected. Splenocytes were positively selected with anti-CD45.1 PE (clone A20) followed by anti-PE microbeads (Miltenyi Biotec), then single HEL-specific GC B cells were sorted on a FACSAria cell sorter as CD45.1$^+$B220$^+$CD19$^+$GL-7$^+$FAS$^+$IgM$^-$IgD$^-$7AAD$^-$ cells directly into 96-well plates. Each well contained the appropriate lysis buffer and RT-PCR mixture: SuperScript III RT (Invitrogen Life Technologies), RNasin Ribonuclease Inhibitor (Promega), dNTPs (GE Healthcare), IGEPAL® CA-630, NP40 (Sigma), and primer CH1IgG-RT (gacacaggatccagagttcc). In order to amplify the specific VH10 IgH variable region, PCR on the obtained cDNA was performed for 50 cycles at 57°C with the PfuUltra II Fusion HS DNA Polymerase (Agilent Technologies) using the following primers: forward primer FW-LVH3-1 (taagtcttctgtacctgttgacag), which binds in the leader region, and reverse primer CH1IgG-PCR (caggggccagtggatagac), which binds in the constant IgG region. All PCR products were visualized on a 1% agarose gel (Sigma) and positive clones were sent to Microsynth AG for sequencing using the FW-LVH3-1 primer.

Quantitative real-time PCR

AID mRNA levels were obtained from FACS sorted HEL-specific GC B cells, distinguished according to the different congenic marker. RNA was obtained using TRIzol LS reagent (Invitrogen), transcribed into cDNA, and analyzed as described before [34], using the as housekeeping gene 18s.

Biocomputing

Translated protein sequences (obtained through ExPASy-Translate tool, http://web.expasy.org/translate/) were aligned to

the HyHEL10 sequence [24] using Clustal Omega (http://www.ebi.ac.uk/Tools/msa/clustalo/). FWR/CDR boundary regions were established using IMGT/V-QUEST [35]. Positive and negative selection values of the FWR/CDR regions were determined with the BASELINe web site (http://selection.med.yale.edu/baseline/). Briefly, sequences were formatted according to the IMGT® numbering scheme (no CDR3) and analyzed using the Mouse Tri-nucleotide as SHM targeting model. Hypermutation patterns were analyzed in a Bayesian framework [26, 27] and p-values were estimated for all the FWR/CDR regions and then mean values from WT, $Cd3e^{-/-}$, Treg-$Cd3e^{-/-}$ sequences were obtained.

Immunohistology

Histological analysis was performed as previously described [8]. The following primary antibodies were used: FITC-conjugated rat anti-mouse GL-7 (BD Biosciences), rat anti-IgD (clone: 11–26c.2a; Biolegend), and mouse anti mouse CD45.1-biotin (clone A20; eBiocience), rat anti-mouse CD35-bio (8C12), IgD-647 (clone: 11–26c.2a), anti-GFP rabbit IgG fraction AF488. Secondary antibodies coupled to AF488, AF594 or AF647 (Molecular Probes) were used. Biotinylated antibodies were amplified with the streptavidin-HRP TSA AF594 or AF647 kits (Molecular Probes). Images were acquired on a confocal Leica TS5 system equipped with a motorized stage or on a Nikon Eclipse E800 microscope with OpenLab software. Images were processed with Photoshop (Adobe) software without non-linear operations.

Statistical analysis

Data were analyzed with Prism 6.04 (GraphPad Software) using the nonparametric unpaired Mann-Whitney U test for comparison of two unpaired groups. For comparison of three or more unpaired groups, the nonparametric Kruskal-Wallis test followed by Dunn's post hoc test were used to calculate of the p value for each group. Graphs show the mean ± SEM. $*p < 0.05$; $**p < 0.01$; $***p < 0.001$. Where not indicated, the p values were not significant.

References

1 **Crotty, S.**, T follicular helper cell differentiation, function, and roles in disease. *Immunity* 2014.**41**: 529–542.

2 **Victora, G. D. and Nussenzweig, M. C.**, Germinal centers. *Annu. Rev. Immunol.* 2012.**30**: 429–457.

3 **Shlomchik, M. J. and Weisel, F.**, Germinal center selection and the development of memory B and plasma cells. *Immunol. Rev.* 2012.**247**: 52–63.

4 **Victora, G. D. and Mesin, L.**, Clonal and cellular dynamics in germinal centers. *Curr. Opin. Immunol.* 2014.**28**: 90–96.

5 **Qi, H., Chen, X., Chu, C., Lu, P., Xu, H. and Yan, J.**, Follicular T-helper cells: controlled localization and cellular interactions. *Immunol. Cell Biol.* 2014.**92**: 28–33.

6 **Baumjohann, D. and Ansel, K. M.**, MicroRNA regulation of the germinal center response. *Curr. Opin. Immunol.* 2014.**28**: 6–11.

7 **Pratama, A. and Vinuesa, C. G.**, Control of TFH cell numbers: why and how?*Immunol. Cell Biol.* 2014.**92**: 40–48.

8 **Baumjohann, D., Preite, S., Reboldi, A., Ronchi, F., Ansel, K. M., Lanzavecchia, A. and Sallusto, F.**, Persistent antigen and germinal center B cells sustain T follicular helper cell responses and phenotype. *Immunity* 2013.**38**: 596–605.

9 **Malissen, M., Gillet, A., Ardouin, L., Bouvier, G., Trucy, J., Ferrier, P., Vivier, E. et al.**, Altered T cell development in mice with a targeted mutation of the CD3-epsilon gene. *EMBO J.* 1995. **14**: 4641–4653.

10 **Radbruch, A., Muehlinghaus, G., Luger, E. O., Inamine, A., Smith, K. G., Dorner, T. and Hiepe, F.**, Competence and competition: the challenge of becoming a long-lived plasma cell. *Nat. Rev. Immunol.* 2006.**6**: 741–750.

11 **Lee, S. K., Rigby, R. J., Zotos, D., Tsai, L. M., Kawamoto, S., Marshall, J. L., Ramiscal, R. R. et al.**, B cell priming for extrafollicular antibody responses requires Bcl-6 expression by T cells. *J. Exp. Med.* 2011.**208**: 1377–1388.

12 **Odegard, J. M., Marks, B. R., DiPlacido, L. D., Poholek, A. C., Kono, D. H., Dong, C., Flavell, R. A. and Craft, J.**, ICOS-dependent extrafollicular helper T cells elicit IgG production via IL-21 in systemic autoimmunity. *J. Exp. Med.* 2008.**205**: 2873–2886.

13 **Victora, G. D., Schwickert, T. A., Fooksman, D. R., Kamphorst, A. O., Meyer-Hermann, M., Dustin, M. L. and Nussenzweig, M. C.**, Germinal center dynamics revealed by multiphoton microscopy with a photoactivatable fluorescent reporter. *Cell* 2010.**143**: 592–605.

14 **Brink, R., Phan, T. G., Paus, D. and Chan, T. D.**, Visualizing the effects of antigen affinity on T-dependent B-cell differentiation. *Immunol. Cell Biol.* 2008.**86**: 31–39.

15 **Chung, Y., Tanaka, S., Chu, F., Nurieva, R. I., Martinez, G. J., Rawal, S., Wang, Y. H. et al.**, Follicular regulatory T cells expressing Foxp3 and Bcl-6 suppress germinal center reactions. *Nat. Med.* 2011.**17**: 983–988.

16 **Linterman, M. A., Pierson, W., Lee, S. K., Kallies, A., Kawamoto, S., Rayner, T. F., Srivastava, M. et al.**, Foxp3+ follicular regulatory T cells control the germinal center response. *Nat. Med.* 2011.**17**: 975–982.

17 **Wollenberg, I., Agua-Doce, A., Hernandez, A., Almeida, C., Oliveira, V. G., Faro, J. and Graca, L.**, Regulation of the germinal center reaction by Foxp3+ follicular regulatory T cells. *J. Immunol.* 2011.**187**: 4553–4560.

18 **Kawamoto, S., Maruya, M., Kato, L. M., Suda, W., Atarashi, K., Doi, Y., Tsutsui, Y. et al.**, Foxp3(+) T cells regulate immunoglobulin a selection and facilitate diversification of bacterial species responsible for immune homeostasis. *Immunity* 2014.**41**: 152–165.

19 **Sakaguchi, S., Vignali, D. A., Rudensky, A. Y., Niec, R. E. and Waldmann, H.**, The plasticity and stability of regulatory T cells. *Nat. Rev. Immunol.* 2013.**13**: 461–467.

20 **Tsuji, M., Komatsu, N., Kawamoto, S., Suzuki, K., Kanagawa, O., Honjo, T., Hori, S. and Fagarasan, S.**, Preferential generation of follicular B helper T cells from Foxp3+ T cells in gut Peyer's patches. *Science* 2009.**323**: 1488–1492.

21 **Sage, P. T., Paterson, A. M., Lovitch, S. B. and Sharpe, A. H.**, The coinhibitory receptor CTLA-4 controls B cell responses by modulating T follicular helper, T follicular regulatory, and T regulatory cells. *Immunity* 2014.**41**: 1026–1039.

22 **Brink, R.**, The imperfect control of self-reactive germinal center B cells. *Curr. Opin. Immunol.* 2014.**28**: 97–101.

23 **Phan, T. G., Grigorova, I., Okada, T. and Cyster, J. G.**, Subcapsular encounter and complement-dependent transport of immune complexes by lymph node B cells. *Nat. Immunol.* 2007. **8**: 992–1000.

24 **Phan, T. G., Gardam, S., Basten, A. and Brink, R.**, Altered migration, recruitment, and somatic hypermutation in the early response of marginal zone B cells to T cell-dependent antigen. *J. Immunol.* 2005.**174**: 4567–4578.

25 **Phan, T. G., Green, J. A., Gray, E. E., Xu, Y. and Cyster, J. G.**, Immune complex relay by subcapsular sinus macrophages and noncognate B cells drives antibody affinity maturation. *Nat. Immunol.* 2009. **10**: 786–793.

26 **Yaari, G., Uduman, M. and Kleinstein, S. H.**, Quantifying selection in high-throughput Immunoglobulin sequencing data sets. *Nucleic Acids Res* 2012.**40**: e134.

27 **Uduman, M., Yaari, G., Hershberg, U., Stern, J. A., Shlomchik, M. J. and Kleinstein, S. H.**, Detecting selection in immunoglobulin sequences. *Nucleic Acids Res.* 2011.**39**: W499–W504.

28 **Sage, P. T., Alvarez, D., Godec, J., von Andrian, U. H. and Sharpe, A. H.**, Circulating T follicular regulatory and helper cells have memory-like properties. *J. Clin. Invest.* 2014. **124**: 5191–5204.

29 **Li, Z., Woo, C. J., Iglesias-Ussel, M. D., Ronai, D. and Scharff, M. D.**, The generation of antibody diversity through somatic hypermutation and class switch recombination. *Genes Dev.* 2004. **18**: 1–11.

30 **Zitvogel, L., Apetoh, L., Ghiringhelli, F., Andre, F., Tesniere, A. and Kroemer, G.**, The anticancer immune response: indispensable for therapeutic success?*J. Clin. Invest.* 2008. **118**: 1991–2001.

31 **Vinuesa, C. G.**, HIV and T follicular helper cells: a dangerous relationship. *J. Clin. Invest.* 2012. **122**: 3059–3062.

32 **Ko, H. J., Yang, H., Yang, J. Y., Seo, S. U., Chang, S. Y., Seong, J. K. and Kweon, M. N.**, Expansion of Tfh-like cells during chronic Salmonella exposure mediates the generation of autoimmune hypergammaglobulinemia in MyD88-deficient mice. *Eur. J. Immunol.* 2012. **42**: 618–628.

33 **Fahey, L. M., Wilson, E. B., Elsaesser, H., Fistonich, C. D., McGavern, D. B. and Brooks, D. G.**, Viral persistence redirects CD4 T cell differentiation toward T follicular helper cells. *J. Exp. Med.* 2011.**208**: 987–999.

34 **Reboldi, A., Coisne, C., Baumjohann, D., Benvenuto, F., Bottinelli, D., Lira, S., Uccelli, A. et al.**, C-C chemokine receptor 6-regulated entry of TH-17 cells into the CNS through the choroid plexus is required for the initiation of EAE. *Nat. Immunol.* 2009. **10**: 514–523.

35 **Brochet, X., Lefranc, M. P. and Giudicelli, V.**, IMGT/V-QUEST: the highly customized and integrated system for IG and TR standardized V-J and V-D-J sequence analysis. *Nucleic Acids Res.* 2008.**36**: W503–W508.

Abbreviations: **AID**: activation-induced cytidine deaminase · **ASC**: antibody-secreting cells · **BCR**: B-cell receptor for antigen · **DZ**: dark zone · **GC**: germinal center · **HEL**: hen egg lysozyme · **LZ**: light zone · **OVA**: ovalbumin · **SHM**: somatic hypermutation · **TCR**: T-cell receptor for antigen · **Tfh**: T follicular helper · **Tfr**: T follicular regulatory

Full correspondence: Dr. Federica Sallusto
Fax: +41-91-820 0305
e-mail: federica.sallusto@irb.usi.ch

Additional correspondence: Dr. Silvia Preite, Institute for Research in Biomedicine, Universita della Svizzera Italiana Bellinzona, Switzerland
e-mail: silvia.preite@irb.usi.ch

Current address: Dirk Baumjohann, Institute for Immunology, Ludwig-Maximilians-Universität München, Munich, Germany;
Francesca Ronchi, Department of Clinical Research, Gastroenterology, University of Bern, Bern, Switzerland